Journal of Magnetism and Magnetic Materials 490 (2019) 165485

Contents lists available at ScienceDirect

Journal of Magnetism and Magnetic Materials

journal homepage: www.elsevier.com/locate/jmmm

Research articles

On the correlation of crystallographic macro-texture and magnetic magnetization anisotropy in non-oriented electrical steel

N. Leuning[a,*], S. Steentjes[b], M. Heller[c], S. Korte-Kerzel[c], K. Hameyer[a]

[a] Institute of Electrical Machines (IEM), RWTH Aachen University, D-52062 Aachen, Germany
[b] Hilti Entwicklungsgesellschaft mbH, D-86916 Kaufering, Germany
[c] Institute of Physical Metallurgy and Metal Physics (IMM), RWTH Aachen University, D-52074 Aachen, Germany

ARTICLE INFO

Keywords:
Electrical steel
Magnetic anisotropy
Anisotropy modeling
Crystallographic texture

ABSTRACT

In material models for the finite-element simulation of electrical machines and the preceding magnetic measurements, the magnetic anisotropy of non-grain oriented electrical steel is usually considered in an over-simplified way, if at all. The magnetization behavior between rolling and transverse direction is not linear and varies with magnetic polarization, a relation that comes in addition to the complexity of the effect. In this paper, the magnetization anisotropy of five industrial non-grain oriented electrical steels is measured with a 1-D single-sheet-tester. The results are evaluated and correlated to the crystallographic texture of the studied materials. An approach to model magnetization curves at 50 Hz in arbitrary directions of the sheet plane is presented. The model is parametrized by measured magnetization curves along three different spatial directions and by macro-texture data in form of an orientation distribution function. This approach leads to a model that replicates the crossing of magnetization curves of different orientations with adequate quantitative accuracy for the application in FE magnetic field simulations.

1. Introduction

Non-grain oriented (NO) electrical steels are used to guide and amplify the magnetic flux, e.g., in rotating electrical machines. Although, the name suggests isotropic magnetic properties, NO steel grades do have a magnetic anisotropy [1–3]. This anisotropy is affected by various factors, e.g., anisotropic grain size, residual mechanical stress from the manufacturing process and the crystallographic texture [4,5]. The dependence of the magnetization behavior on the crystallographic texture is related to the magneto-crystalline anisotropy of the body-centered-cubic (bcc) iron single crystal [6]. Different magnetic field strengths are needed to magnetize the material along different spatial directions, i.e., the cube edges [1 0 0] (easy axes) are easier to magnetize than the surface-diagonals [1 1 0] (medium axes) and space-diagonals [1 1 1] (hard axes) [7–9].

Polycrystalline materials, such as NO FeSi, are composed of grains as distinct areas in which a single crystallographic orientation is maintained i.e., each grain has a distinct orientation relative to the adjacent grains. The distribution of orientations of a polycrystalline material can be expressed by its crystallographic texture [10,3]. In most materials, certain orientations are more frequent than others, which can be one of the reasons for the technical applications of said materials. One example is the sharp texture of grain oriented (GO) electrical steel which is applied in transformers, where the magnetic flux is primarily alternating along the easy axes. Texture evolution takes place during production and processing of electrical steel [11–13]. Chemistry, as well as hot-rolling, cold-rolling and annealing conditions directly affect the resulting texture [12–14]. For GO, the required Goss-texture can be achieved within tight tolerances. For NO this is not the case. Best possible magnetization with consideration of the entire sheet plane should be obtained with a texture distribution of a maximum share of easy magnetization axes, statistically distributed in the sheet plane [8,14]. Due to its application in rotating electrical machines, NO is meant to provide homogeneous magnetization behavior in each direction of the sheet plane; to counter the round geometry and the local presence of rotating magnetic field loci [15,16]. With conventional production routes, the varieties in texture of NO are relatively low and generally it is far from this desired texture [12].

The texture is a source of anisotropy that is estimated to be dominant at medium to high values of magnetic polarizations. In this range, magnetization increases mostly by domain rotation [7,9,17]. The previously restructured and grown domains, which likely are grown in favorable orientations close to easy directions, align along the external field and have to be diverted from the easy axes, thereby being directly

* Corresponding author.
E-mail address: nora.leuning@iem.rwth-aachen.de (N. Leuning).

https://doi.org/10.1016/j.jmmm.2019.165485
Received 24 May 2019; Received in revised form 21 June 2019; Accepted 21 June 2019
Available online 02 July 2019
0304-8853/

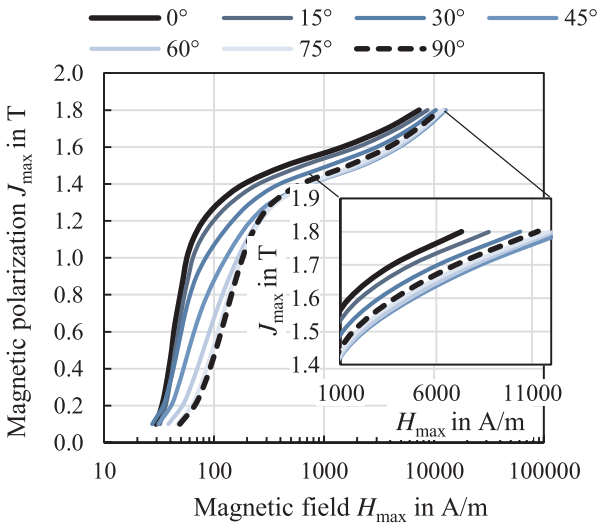

(a) Magnetization curves of a M270-50A at 50 Hz in different angles relative to RD.

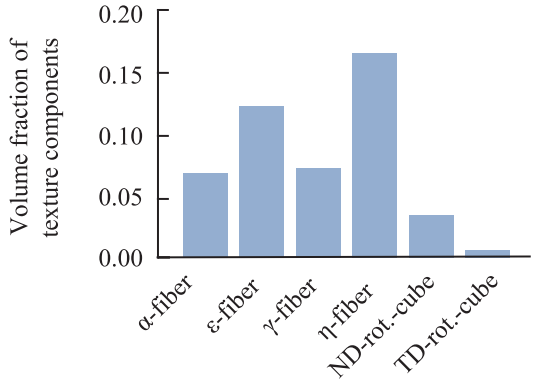

(b) Volume fraction of texture components of a M270-50A, by pole figure measurements with XRD.

Fig. 1. Magnetic and crystallographic anisotropy of a non-oriented electrical steel (M270-50A).

linked to the crystallographic texture. At low to medium magnetic polarizations the magnetization process is driven by domain wall pinning and motion [7,9,17]. Here, micro-structural features, such as grain size, grain morphology, precipitations and mechanical stress govern the magnetization behavior. The saturation magnetization solely depends on the chemical composition and, thereby, anisotropy is eliminated in saturation. As a result of these aforementioned relations, the magnetic anisotropy is not constant throughout the magnetization process. As depicted in Fig. 1 (a), this can lead to a crossing of magnetization curves, measured in various directions relative to the rolling direction (RD) of the same material, where neither transverse direction (TD), nor 55° is solely the hardest magnetization direction. Fig. 1 (b) gives information on the accompanying volume fractions of selected texture components, in this case of relevant fibers for electrical steels, of the M270-50A of Fig. 1 (a). In texture characterization, fibers comprise in some way related orientations. The γ-fiber for example comprises all orientations with [1 1 1]-directions ∥ to the normal direction (ND) of the sheet. A schematic illustration is given in Fig. 2 (a). Consequently, this fiber, due to the cubic geometry, results in the largest possible share of hard magnetization axes in the sheet plane. The on the other hand, previously described desired NO texture is depicted in Fig. 2 (b). Here, all orientations have an [1 0 0] axis ∥ to ND which results in a maximum number of easy magnetization axes in the sheet plane. Visually, this

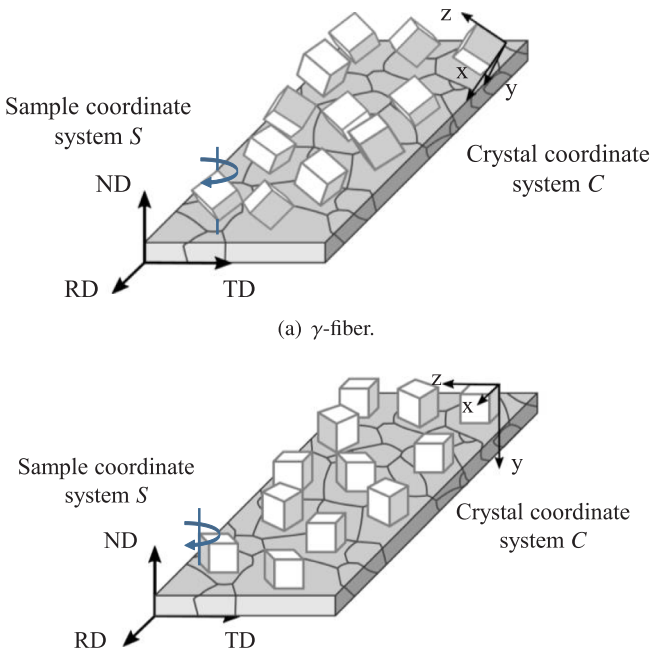

(a) γ-fiber.

(b) ND-rotated cube fiber.

Fig. 2. Schematic illustration of crystallographic fibers.

corresponds to cubes with a parallel plane to the RD-TD-plane, which is rotated around ND, hence the name ND-rotated cube fiber, but also called θ fiber. Analysis of fiber components enables general comparisons of different textures. The ratio of γ- to θ-fiber, also called texture factor TF, as used for example by [16], aims to evaluate the texture of electrical steel. Although, the general magnetization behavior of NO can be linked with texture and compared, however, the TF does not allow conclusions on the anisotropy, because it includes only two fibers instead of all orientations.

In this paper, the correlation of crystallographic macro-texture and magnetic magnetization anisotropy in five industrial NO electrical steels is presented. The magnetization behavior along different in-plane directions is studied, in order to improve the physical understanding of the orientation dependence of the magnetization behavior. Furthermore, an approach to model the magnetization in arbitrary spatial orientations between RD and TD at 50 Hz is presented. This model is based on a limited number of magnetic measurements, i.e., magnetization curves measured in three directions and crystallographic texture. Due to the low effort, the model can applied to consider in finite-element (FE) machine simulations for a consideration of anisotropic material behavior.

2. Experimental

The magnetic measurements for the presented study are conducted with a single-sheet-tester (SST) and Brockhaus measurement systems MPG200. For a detailed characterization of the magnetic anisotropy 120 mm x 120 mm rectangular samples are cut in 5°-angles between RD and TD. The samples are measured with a magnetizing frequency of 50 Hz in 0.1 T-steps up to 1.8 T. In this experimental setup, the primary induction coil is placed on top of the secondary measuring coil, which is used to trace the induced voltage. The current in the primary windings, creates a magnetic field (current-driven) perpendicular to the winding system. Under the assumption that demagnetizing effects are neglected, this H-field is not affected if a ferromagnetic sample is placed inside this winding system. The resulting B however, is not considered correctly in such an SST. Considering the vectorial properties of B and H, this SST-setup holds a systematic error. Only the components perpendicular to

the windings can be considered. The vector components parallel to the windings are neglected. The absolute $B_{abs.}$ can thus, be higher, than the one measured with the SST. This is a known problem but the SST is still a conventional measurement device for magnetic properties of electrical steel and as will be presented, it is sufficient for the desired correlation and modeling approaches on the magnetic aniostropy of NO.

For the correlation of the crystallographic texture with the magnetic anisotropy, the orientation distribution function ODF of the crystallographic macro-texture, obtained by X-ray diffraction (XRD), is evaluated in the middle of the sheet's cross section. Considering the XRD measurements, a Bruker D8 Advanced goniometer with a HI-STAR area detector and Fe-radiation at 30 kV an 25 mA was utilized. The macro-texture gives information on the global properties, i.e., the intensity of different orientations of a sample, instead of localized information for example by electron backscatter diffraction (EBSD) of micro-texture analysis. The sample size is approximately 10×12 mm^2. The maximum grain size of the studied materials is 130 μm, so that in all materials, a sufficient number of grains is measured to ensure that the macro-texture represents the overall texture of the material.

The so-called A-parameter, in the following also described as A_θ, introduced in [3] is used to quantify the texture magnetically. The parameter A_θ is an indicator for the magnetization behavior and can be calculated using solely the ODF. In Fig. 3, a schematic description is displayed, where θ is the angle between the magnetization vector $\vec{M}$ and the RD of the sample, i.e., the direction of the sheet plane the sample is magnetized. $A_\theta(g)$ describes the mean angle between $\vec{M}$ and the closest easy magnetization direction of one crystal. For a polycrystalline material A_θ is an orientation-averaged value, considering all orientations $f(g)$ of the entire sample as followed:

$$A_\theta = \int f(g) A_\theta(g) \mathrm{d}g. \tag{1}$$

Lower values for A suggest that more easy axes are aligned in or are closer to the direction of magnetization. The A-parameter has been used in various scientific publications to account for the texture influence of NO [7,9,12,14,18].

The five studied materials are all conventional, industrial NO electrical steel with a silicon content above 2.2 wt%. This means no phase transition occurs during the production process. The thicknesses, mean grain diameter and alloying content of Silicon and Aluminum are presented in Table 1.

3. Results and discussion

3.1. Texture analysis

A comparison between the crystallographic texture of the five studied materials reveals certain similarities. The description of texture in the following secction follows the Bunge notation [10]. Orientations can be characterized by the three Euler-angles φ_1, Φ and φ_2 which translate the crystal coordinate system to the sample coordinate system

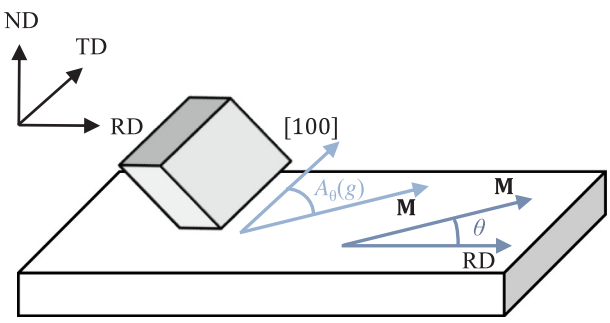

Fig. 3. Schematic description of the A-parameter according to [3].

Table 1
Nominal thickness, chemical composition, mean grain diameter D of the studied materials.

	Thickness	wt% Si	wt% Al	D in µm
Material 1	0.35 mm	3.32	0.76	105
Material 2	0.20 mm	3.77	0.89	92
Material 3	0.27 mm	3.16	1.23	97
Material 4	0.27 mm	3.39	1.50	107
Material 5	0.23 mm	3.64	0.23	65

by three consecutive rotations and therby describe the relative orientation of the crystal to the sample geometry. In Fig. 4, the $\varphi_2 = 45°$ sections of the ODF are presented along with the calculated A-parameters between RD (0°) and TD (90°). This ODF section is commonly used for the analysis of electrical steel textures, because the most relevant orientations and fibers can all be found here. Rotated cube orientations, especially Cube, Cube-ND 22.5, and Cube-ND 45, the γ-fiber and the Goss-orientation have notable intensities in these electrical steels. From the observations, two types of electrical steel textures can be distinguished. Textures with a single strong maximum of the A-parameter at about 55°, which is linked to the Goss texture component and textures with two more or less pronounced maxima at about 30° and 60° and a less steady trend.

Some other general observations can be made for the studied materials, as well as from other scientific literature. First, the A-parameter in RD is always lower than in TD. Material 3 has the lowest A-parameter with 27.3°. In previous work on thicker material, i.e., above 0.3 mm similar parameter ranges were presented for industrial NO with the lowest A-parameter of 25.9° [18]. The authors of [14], obtained values for A of about 24° for conventional hot rolling and 25.5° for asymetric hot rolling of a 2.3 wt% Si NO in RD.

If looking at the shape of the curve of the A-parameter, the graphs of material 2, 3 and 4 in Fig. 4 are similar to results presented in [14] and material M270-50A of [18], where the peak value is between 45° and 60°. The magnetization direction of 55° is often characterized as the hardest magnetization direction.This is generally related to the Goss-texture, which is typical for GO, however also occurs in NO. In the $\varphi_2 = 45°$ section, the Goss-orientation is in the bottom right corner. For the studied NOs a higher intensity in the bottom right corner can be obeserved for material 2, 3 and 4. In this orientation the cube is sitting on one edge so that this edge is directed parallel to RD. Thus, in TD the magnetization direction is along a surface diagonal. Due to the geometric constraints, the hardest magnetization direction in the sheet plane for this component is 55°. In [1], a similar course of the decreasing magnetic polarization has been observed, which the authors also relate to this orientation.

Material 1 and 5 have less pronounced maxima of the A-parameter and more Cube-ND 22.5 components. In [18] this is also observed for an M330-50A. For NO, the most unfavorable orientation distribution is the γ-fiber. In the $\varphi_2 = 45°$ section, this is highlighted by intensities around $\Phi = 55°$ and $\varphi_1 = 0°$ to 90°. With this fiber, hard magnetization axes are distributed in the sheet plane. Material 1, 2 and 5 all have intensity along this γ-fiber. Especially material 2, which also has the highest value for the total A-parameter. The γ-fiber is a typical rolling texture for FeSi and, thus, is difficult to avoid during conventional production of NO.

Although the course of the A-parameter can be differentiated into two different types, the averaged parameter of all directions A_{total} for the materials does not follow a specific trend that could be linked to either sheet thickness or silicon content but is rather similar for all materials, as depicted in Table 2. Presented is the mean value considering the calculated A_θ in 5°-steps. Material 1 hast the lowest value, whereas material 2 has the highest. The observed parameters are in a range of 30 to 33 and, thereby, in a range similar to other work [3,14].

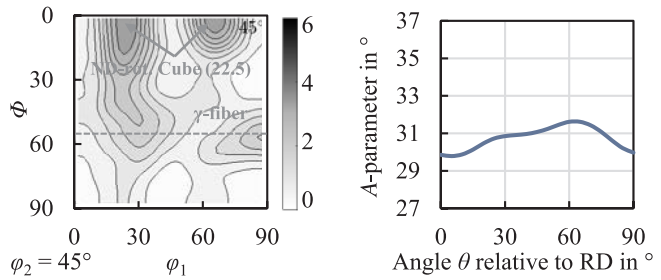

(a) Material 1

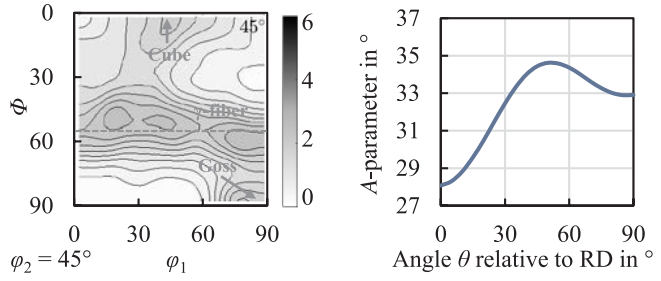

(b) Material 2

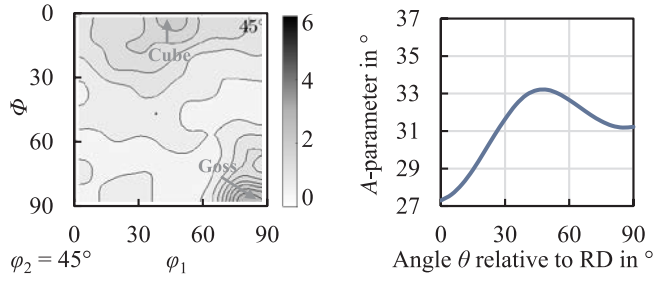

(c) Material 3

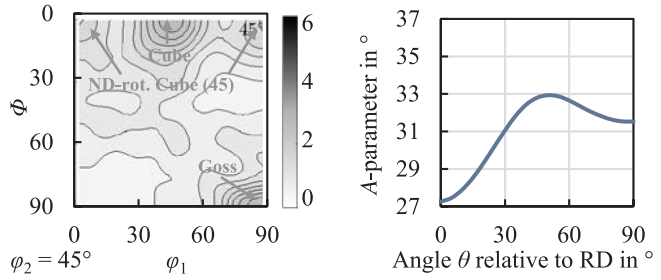

(d) Material 4

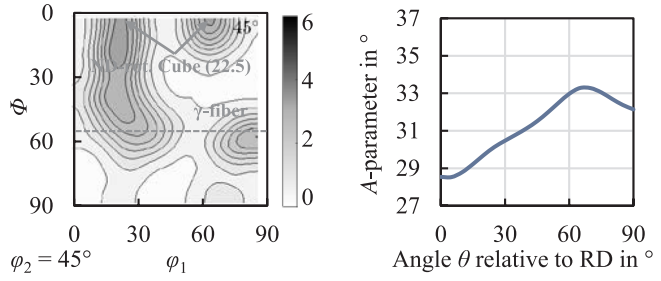

(e) Material 5

Fig. 4. ODF sections (Bunge notation) and calculated *A*-parameter for the five studied materials with higlighting of respective dominant texture components.

Table 2
Directional averaged *A*-parameter of the studied materials.

Material	1	2	3	4	5
A_{total}	30.7	32.2	31.3	30.9	31.2

3.2. Modeling of magnetization anisotropy considering texture and correlation

Due to the dependency of the magnetization behavior on the crystallographic texture, the *A*-parameter who in theory links both, is possible to be adapted to model the magnetic anisotropy. Other correlation approaches focus on the anisotropy energy, as presented in [1,2,19]. The benefits of the approach presented in this paper, is the low measurement effort and low overall effort to model the anisotropy for arbitrary magnetization directions in the sheet plane. In previous work, a qualitative correlation between the crystallographic texture and the magnetization at 1.5 T has been shown [18]. The aim of the model is to reproduce magnetization curves at 50 Hz in arbitrary spatial directions θ for all polarizations J that have been used in the magnetic measurements, i.e., in this case 0.1 T to 1.8 T in 0.1 T-steps. The model is a combination of an elliptical model and a texture model.

The texture model for the magnetic field H_{texture}, is based on the spatial course of the *A*-parameter over the range of $\theta = 0°$ to 90°. The theoretically required field H_{texture} for a polarization J at an angle θ can be expressed as the required field in RD, plus an angular dependent increase or decrease of the magnetic field ΔH_θ,

$$H_{\text{texture}}(\theta, J) = H_{\text{RD}}(J) + \Delta H_\theta(J). \tag{2}$$

For this, *A* has to be translated to the dimensional unit of a magnetic field, i.e., A/m. This can be obtained by a simple scaling approach (3), where the course of the *A*-parameter is scaled to the RD and TD magnetic measurements of a material,

$$\Delta H_\theta(J) = A_\theta\left(\frac{\Delta H_{\text{scale}}(J)}{\Delta A_{\text{scale}}(J)}\right) - A_{\text{RD}}\left(\frac{\Delta H_{\text{scale}}(J)}{\Delta A_{\text{scale}}(J)}\right), \tag{3}$$

where the minuend sets the range of the *A*-parameter to the range of H_{RD} and H_{TD} for each polarization J and, thereby, to the unit of A/m. The subtrahend scales the value to the RD measurement, so that $\Delta H_\theta(J)$ is the additional field strength required to magnetize the material in another spatial direction θ relative to RD. For (3), ΔH and ΔA are defined as follows,

$$\Delta H_{\text{scale}}(J) = |H_{\text{TD}}(J) - H_{\text{RD}}(J)|, \tag{4}$$

$$\Delta A_{\text{scale}} = |A_{\text{TD}} - A_{\text{RD}}|. \tag{5}$$

The course of the *A*-parameter can easily be described by a mathematical function. Due to the fact that the parameter is calculated from the ODF, the number of setpoints for an interpolation can be chosen in incremental steps, if necessary. Empirically, polynomial functions are able to describe the spatial curve with low overall error ($R^2 > 0.99$). As a result, the required magnetic field for any given direction θ can be modeled.

The influence of texture is not estimated to be alike for all polarization levels of a magnetization curve. As [7,9] have noted, the texture affects the domain rotation process at medium to high magnetic polarizations. Consequently, a texture based model should perform best in this range.

The second part of the model is based on the elliptical model described in [20]. Here, the magnetic field locus is modeled as an ellipse in the RD-TD plane with x and y coordinates for each J. The mathematical description for an ellipse is,

$$\frac{H_{x,J}^2}{b^2} + \frac{H_{y,J}^2}{a^2} = 1, \tag{6}$$

where

$$b^2 = \frac{J_{RD}^2}{\mu_{RD}^2} \text{ and } a^2 = \frac{J_{TD}^2}{\mu_{TD}^2} \tag{7}$$

are obtained from the RD and TD measurements with μ_{RD} and μ_{TD} being the permeability of the material in the principle directions RD and TD. In order to transfer the elliptical model from the H_x-H_y-plane to $H(\theta)$, trigonometrical relations can be used, as for example,

$$H_{elliptical} = \frac{H_x(\theta)}{\cos\theta}. \tag{8}$$

Originally, this model has been introduced as a 2-D magnetic field calculation approach for the consideration of anisotropic, nonlinear magnetization behavior of GO. In this study, this elliptical model is proposed to account for the magnetization behavior of NO at low to medium polarization levels, where the domain rotation is not the dominant magnetization process, but the domain wall movement and pinning. The associated influences are the grain structure, with grain boundaries as obstacles for the free domain wall movements, precipitations, which also cause pinning and mechanical residual stress.

Due to the circumstance that the introduced texture and elliptical models are expected to only apply for a certain magnetic polarization range, a combination of both models is now introduced. With this approach, the entire range of a magnetization curve between 0.1 T and 1.8 T can be modeled and a theoretical $H_{mod.}$ for any direction θ relative to RD can be determined. In Eq. (9), w is a weighting factor to balance the elliptical $H_{elliptical}$ as well as the texture $H_{texture}$ contribution.

$$H_{mod.}(J, \theta) = w \cdot H_{texture} + (1 - w) \cdot H_{elliptical}, \tag{9}$$

with

$$w, \text{ so that } |H_{55°,meas.} - H_{55°,mod.}| \rightarrow \min.. \tag{10}$$

An additional magnetic measurement in 55° serves as means to improve the fit by weighting the parts of $H_{elliptical}$ and $H_{texture}$ and amplifying the influence of texture for each polarization J. The weighting factor w is not limited to the range between 0 and 1. Although w differs for the materials, a trend can be observed. Up to 0.6 T, 0.7 T, w stays almost constant. From this point up to 1.2 T, w increases. At 1.3 T, 1.4 T w increases abruptly, before decreasing slightly. The course of w for the materials is displayed in Fig. 6. Material 1 differs from the other materials slightly in the course and the range of the factor w, as highlighted.

In Fig. 5, results of this modeling approach are displayed exemplary for material 4. Fig. 5 (a) at 0.3 T represents low inductions, with a $w = 0.13$ and resulting high share of the elliptical component, whereas Fig. 5 (b) represents higher magnetic polarizations of 1.7 T, where the texture is dominant and a weighting factor of $w = 2.2$ is observed. The model is parametrized only by the RD, TD measurements and the ODF. The 55° measurement is used to find w.

3.3. Comparison of modeling results and measurements

Results for the model Eq. (9), parametrized with said magnetic measurements as well as the crystallographic macro-texture in form of an ODF and weighted, are now presented and compared to actual measurements. For this purpose, additional magnetic measurements of intermediate orientations in $\theta = 5°$-steps between RD and TD are obtained.

In Fig. 7, results of this comparison for the studied materials are displayed from 1.5 T up to 1.7 T. For all materials, the comparison of $H_{meas.}$ and $H_{mod.}$ shows good accordance. The distinct spatial courses of the curves can be reproduced, with a strong maximum for material 2, 3 and 4 and a different course for material 1 and 4. However, it is noticeable, that the measurement results slightly scatter. This unsteadiness likely stems from measurement uncertainties more than actual effects, for example the measurement of $\theta = 85°$ for material 2, which is

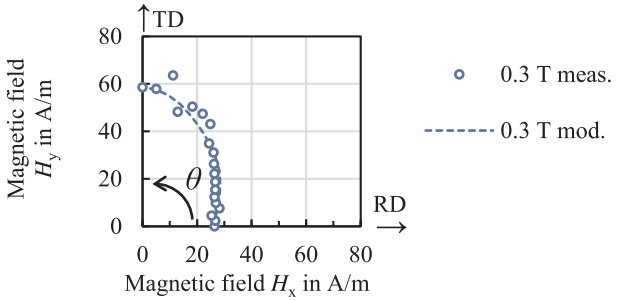

(a) Theoretical results with higher elliptical share at low polarizations, with $w = 0.13$

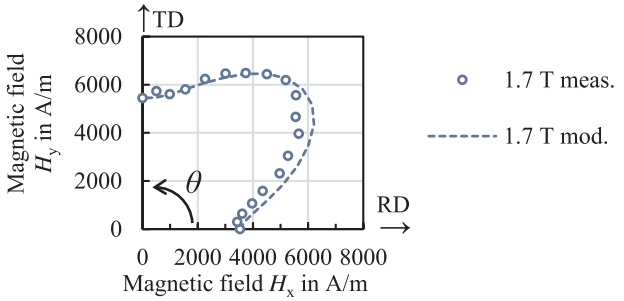

(b) Theoretical results with higher texture share at higher polarizations, with $w = 2.2$

Fig. 5. Comparison of theoretical Eq. (9) and measured magnetic field H at 0.3 T and 1.7 T for material 4 presented in the H_x-H_y space.

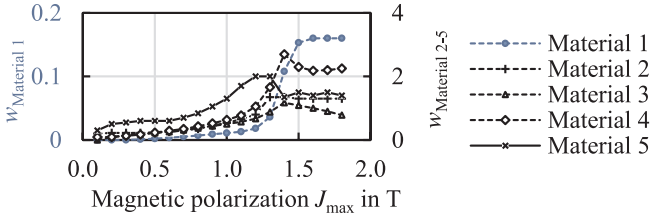

Fig. 6. Weighting factor w for all five materials.

likely an outlier compared with the measurements of adjacent spatial directions. As displayed in Fig. 6, the share of the texture component to the model is dominant at high polarizations. Due to the good accordance of measurement and theoretical results, this actually confirms that in this region of domain rotation, the crystallographic texture is the dominant source of anisotropy in NO.

At lower magnetic polarizations, there is a higher share of the elliptical contribution. In this region, the magnetization process is linked to domain wall pinning and mechanical stress. The region of around 1.0 T, as displayed in Fig. 8 has components of both, the elliptical as well as the texture model. For the magnetization curves, this means that there is more or less a continuous increase of required magnetic field with spatial direction from RD to TD. At higher magnetic polarization, where the texture is dominant, intermediate directions can become the hardest to magnetize. Consequently, a crossing of magnetization curves must occur for certain materials in the region, where the texture becomes dominant. In Fig. 9, results obtained by the presented approach are displayed for 50 Hz alongside measurements for the entire magnetization curve for all materials for exemplary directions of 15°, 50° and 85° relative to RD. The crossing of the magnetization curves as well as the total anisotropy are in good accordance. Between the materials, material 5 has the lowest overall anisotropy, followed by material 2. Materials 1, 3 and 4 have a high anisotropy. Furthermore the 15° magnetization curve displays the easiest magnetization behavior at all polarization levels. A crossing occurs for the 50° and 85° curves.

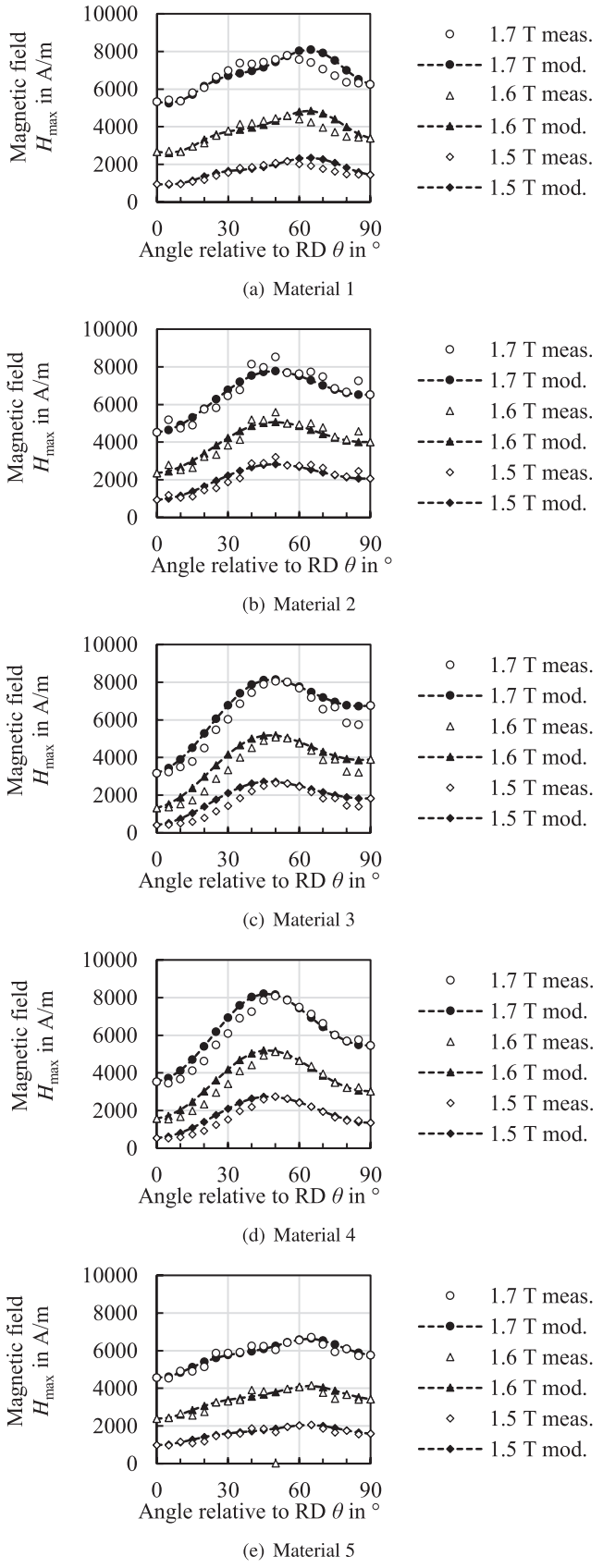

Fig. 7. Measured and theoretical Eq. (9) magnetic field loci for different magnetic polarizations of 1.5 T, 1.6 T and 1.7 T between RD and TD for the five studied materials.

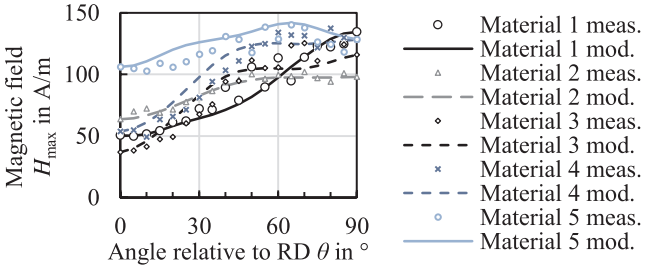

Fig. 8. Measured and theoretical Eq. (9) magnetic field for 1.0 T between RD and TD for the five studied materials.

In Fig. 10 the relative error between the measured and theoretical results for all angles θ at 1.8 T are displayed. For the presented approach, i.e., Eq. (9), the error at this magnetic polarization is in the range of ± 10% (Fig. 10 (a)). As mentioned earlier, one reason for this error can be the quality of the measurements and resulting measurements errors due to material fluctuation for the different samples, i.e., offset of angle θ, fluctuation of geometrical dimensions or inhomogeneities. Therefore, the models sometimes over- and sometimes underestimates the actual required magnetic field. Compared with the solely elliptical approach, however, the approach has a significantly higher accuracy. In Fig. 10 (b), the relative error at 1.8 T is displayed for the elliptical model. For all studied materials, the error between 30° and 60° is between −10% and −60%. The reason for this is that the hardest magnetization axes are not considered in this approach. In accordance with the previous results, a high error at medium to high polarization with the elliptical model is expected, because of the neglect of the physical relation between domain rotation at higher magnetic polarizations and the crystallographic texture. Consequently, this is the strength of the presented approach.

Another point that has to be discussed is the disregard of vectorial properties of J and H with this approach. For 1-D measurements on a SST, J and H are often considered to be collinear. However, this is not necessarily the case due to the alignment of the J vector with the magnetic domain structure of the material. In the SST setup, a primary coil generates the magnetic field in x-direction. At low magnetic fields, favorable oriented domains grow. These domains are not necessarily aligned to the direction x, which leads to a vector J in a different direction than H. With the secondary winding that picks up the inducted voltage sitting below the primary winding, only the x-component of the J vector is considered. Because the domain reorientation and rotation processes are occurring consecutively the direction of the resulting J relative to H is dependent on the excitation as well. At higher inductions of > 1.5 T, the vectors are approximating collinearity. Even though the vector properties are not considered, the presented approach leads to good results. With additional consideration of the phase angle between the vectors of J and H, i.e., θ_{HJ} and understanding of its characteristic, the approach could enable a further consideration of vectorial properties. However a rotational single-sheet-tester (RSST) setup would be required for an in-depth study.

4. Conclusions

During standardized material characterizations with SST and Epstein-frame (EF), the material is tested generally in rolling (RD) and transverse (TD) direction only, or in case of EFs with a mixed sample set of RD and TD samples. When this data is pre-processed for FE machine simulations, the anisotropy is rarely considered. Linear or solely elliptical simplification are not sufficient to be used for a more detailed description of magnetization behavior in the entire lamination sheet plane, due to the crossing of magnetization curves at medium polarizations for some spatial directions. In this study, the anisotropy of five different industrial NO has been studied and an approach to determine

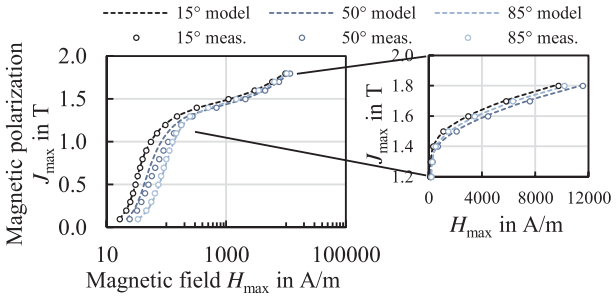

(a) Material 1

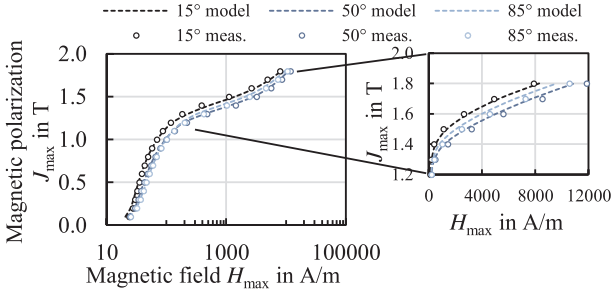

(b) Material 2

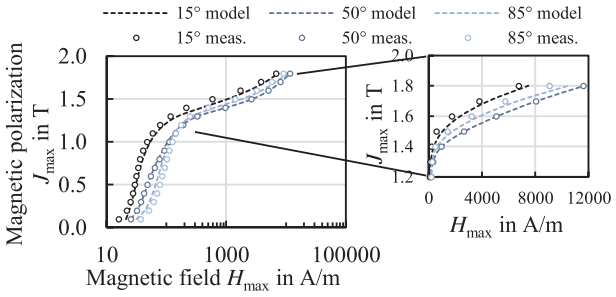

(c) Material 4

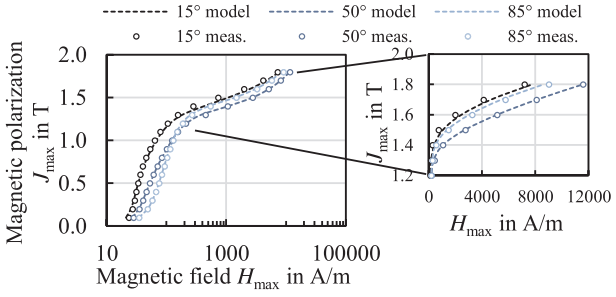

(d) Material 5

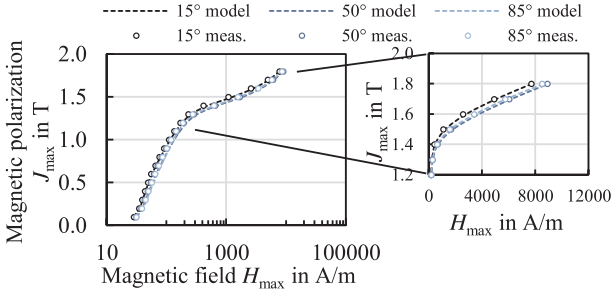

(e) Material 3

Fig. 9. Theoretical Eq. (9) and measured magnetization curves at 50 Hz for θ of 15°, 55° and 85° relative to RD.

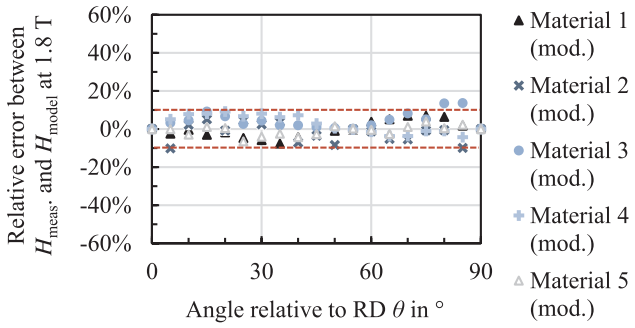

(a) Model

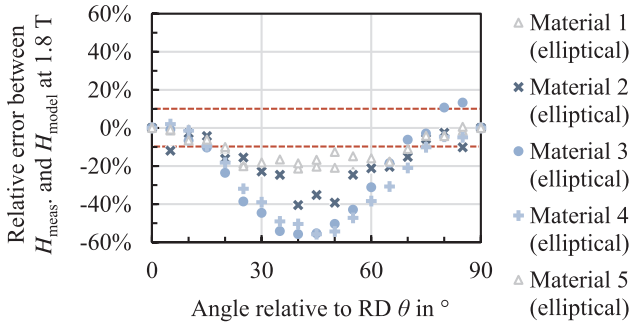

(b) Solely elliptical model

Fig. 10. Relative error between measured and modeled field strength H_{max} for the presented model and comparison to solely elliptical model at 1.8 T for all five materials, with the ± 10% mark highlighted.

the theoretical magnetization curve in arbitrary directions of the sheet plane, based on magnetic measurements in only three spatial directions, as well as a ODF measurements has been presented. The key findings can be summarized as follows:

- There are typical textures in NO that mostly comprise shares of Goss-orientation, rotated Cube orientations and γ-fiber. The *A*-parameter can be utilized to comprehensively describe the estimated effect of texture on the magnetization behavior. The shape of the *A*-parameter curve can be used to parametrize a texture model.
- Due to the comparison of calculated and measured results, it has been found that the texture is dominant for the anisotropy of NO at medium to high magnetic polarizations above 1.3 T. At low polarizations, the magnetization behavior is affected by other parameters, likely the grain structure and mechanical stress that affects the domain wall motion. This results in a continual anisotropy in the sheet plane, i.e., elliptical behavior.
- The presented approach of a combination of an elliptical and a texture model leads to good results to determine magnetization curves of various spatial orientations θ. The model is parametrized with magnetization curves along RD and TD, along with and ODF and complemented with a weighting factor w based on an additional measurement at 55°.
- With the presented approach, the magnetization curves for all studied materials could be predicted in good agreement with experimental measurements. Even the crossing of magnetization curves of certain directions was reproduced, even though the measurement results of these orientation had not been included for the parametrization.

The study has been performed at a frequency of 50 Hz. Further frequencies as well as the consideration of vectorial properties will be studied in further work.

Acknowledgement

This work is funded by the Deutsche Forschungsgemeinschaft (DFG, German Research Foundation) 255713208, 218259799 and carried out in the research group project “FOR 1897 Low-Loss Electrical Steel for Energy-Efficient Electrical Drives”.

References

[1] F.J.G. Landgraf, T. Yonamine, M. Emura, M.A. Cunha, Modelling the angular dependence of magnetic properties of a fully processed non-oriented electrical steel, J. Magn. Magn. Mater. 254–255 (2003) 328–330, https://doi.org/10.1016/S0304-8853(02)00827-2.

[2] H.G. Kang, K.M. Lee, M.Y. Huh, J.S. Kim, J.T. Park, O. Engler, Quantification of magnetic flux density in non-oriented electrical steel sheets by analysis of texture components, J. Magn. Magn. Mater. 323 (17) (2011) 2248–2253, https://doi.org/10.1016/j.jmmm.2011.03.041.

[3] L. Kestens, S. Jacobs, Texture control during the manufacturing of nonoriented electrical steels, Texture Stress, Microstruct. (2008) 1–9, https://doi.org/10.1155/2008/173083.

[4] M. Emura, M.F. de Campos, F.J.G. Landgraf, J.C. Teixeira, Angular dependence of magnetic properties of 2% silicon electrical steel, J. Magn. Magn. Mater. 226–230 (2001) 1524–1526, https://doi.org/10.1016/S0304-8853(00)00946-X.

[5] N. Leuning, S. Steentjes, K. Hameyer, Effect of grain size and magnetic texture on iron-loss components in NO electrical steel at different frequencies, J. Magn. Magn. Mater. 469 (2019) 373–382, https://doi.org/10.1016/j.jmmm.2018.07.073.

[6] R.M. Bozorth, Ferromagnetism, Van Nostrand, 1951.

[7] J. Barros, J. Schneider, K. Verbeken, Y. Houbaert, On the correlation between microstructure and magnetic losses in electrical steel, J. Magn. Magn. Mater. 320 (20) (2008) 2490–2493, https://doi.org/10.1016/j.jmmm.2008.04.056.

[8] K. Verbeken, J. Schneider, J. Verstraete, H. Hermann, Y. Houbaert, Effect of hot and cold rolling on grain size and texture in Fe-2.4wt%si strips, IEEE Trans. Magn. 44 (11) (2008) 3820–3823, https://doi.org/10.1109/TMAG.2008.2001318.

[9] E. Gomes, J. Schneider, K. Verbeken, J. Barros, Y. Houbaert, Correlation between microstructure, texture, and magnetic induction in nonoriented electrical steels, IEEE Trans. Magn. 46 (2) (2010) 310–313, https://doi.org/10.1109/TMAG.2009.2032425.

[10] H.-J. Bunge, Texture Analysis in Materials Science, Elsevier (1982), https://doi.org/10.1016/C2013-0-11769-2.

[11] M.Z. Salih, M. Uhlarz, F. Pyczak, H.G. Brokmeier, B. Weidenfeller, N. Al-hamdany, W.M. Gan, Z.Y. Zhong, N. Schell, The effect of magnetic annealing on crystallographic texture and magnetic properties of fe-2.6% si, J. Magn. Magn. Mater. 381 (2015) 350–359, https://doi.org/10.1016/j.jmmm.2015.01.004.

[12] Y. He, E.J. Hilinski, Texture and magnetic properties of non-oriented electrical steels processed by an unconventional cold rolling scheme, J. Magn. Magn. Mater. 405 (2016) 337–352, https://doi.org/10.1016/j.jmmm.2015.12.057.

[13] N. Leuning, S. Steentjes, A. Stcker, R. Kawalla, X. Wei, J. Dierdorf, G. Hirt, S. Roggenbuck, S. Korte-Kerzel, H.A. Weiss, W. Volk, K. Hameyer, Impact of the interaction of material production and mechanical processing on the magnetic properties of non-oriented electrical steel, AIP Adv. 8 (4) (2018) 047601, , https://doi.org/10.1063/1.4994143.

[14] S. Chen, J. Butler, S. Melzer, Effect of asymmetric hot rolling on texture, microstructure and magnetic properties in a non-grain oriented electrical steel, J. Magn. Magn. Mater. 368 (2014) 342–352, https://doi.org/10.1016/j.jmmm.2014.05.054.

[15] A. Thul, S. Steentjes, B. Schauerte, P. Klimczyk, P. Denke, K. Hameyer, Rotating Magnetizations in Electrical Machines: Measurements and Modelling, in: 62nd Annual Conference on Magnetism and Magnetic Materials, MMM 2017, Pallavi Dhagat, Pittsburgh, Pennsylvania, USA, 2017, pp. 419–420.

[16] P. Ghosh, R.R. Chromik, B. Vaseghi, A.M. Knight, Effect of crystallographic texture on the bulk magnetic properties of non-oriented electrical steels, J. Magn. Magn. Mater. 365 (2014–09) (2014) 14–22, https://doi.org/10.1016/j.jmmm.2014.04.051.

[17] D.C. Jiles, Introduction to Magnetism and Magnetic Materials, Second Edition, CRC Press, 1998.

[18] N. Leuning, S. Steentjes, K. Hameyer, On the homogeneity and isotropy of non-grain-oriented electrical steel sheets for the modeling of basic magnetic properties from microstructure and texture, IEEE Trans. Magn. 53 (11) (2017) 1–5, https://doi.org/10.1109/TMAG.2017.2701508.

[19] T. Yonamine, F.J.G. Landgraf, Correlation between magnetic properties and crystallographic texture of silicon steel, J. Magn. Magn. Mater. 272–276 (Supplement) (2004) E565–E566.

[20] J. Dedulle, G. Meunier, A. Foggia, J. Sabonnadiere, D. Shen, Magnetic fields in nonlinear anisotropic grain-oriented iron-sheet, IEEE Trans. Magn. 26 (1990) 524–527, https://doi.org/10.1109/20.106369.